ACS APPLIED POLYMER MATERIALS

pubs.acs.org/acsapm
Article

Upcycling Plastic Waste into Sulfonated PET Ion Exchange Membranes for Redox Flow Batteries

Marco Morelli,[§] Varun Donnakatte Neelalochana,[§] Vivek Manish, Alda MP Simões, Maria F. Pantano, Paolo Scardi, and Narges Ataollahi*

Cite This: ACS Appl. Polym. Mater. 2026, 8, 2653−2661

ABSTRACT: The development of low-cost, sustainable, and fluorine-free proton exchange membranes (PEMs) is vital for enabling scalable vanadium redox flow battery (VRFB) technologies. In this work, we report the use of sulfonated polyethylene terephthalate (sPET) membranes, synthesized via chemical modification of recycled PET waste bottles, as a viable alternative to conventional Nafion. The sPET membrane demonstrated competitive electrochemical performance, with charge−discharge cycling confirming stable operation at moderate current densities and Coulombic efficiencies ranging from 66% to 80%. Electrochemical impedance spectroscopy revealed comparable charge transfer resistance to Nafion (31 vs 30 mΩ), especially under dynamic flow conditions. Despite slightly lower ionic conductivity and greater ohmic losses under stagnant conditions, the sPET membrane exhibited acceptable voltage and energy efficiencies (up to 59%), validating its applicability for energy storage systems. These results showcase sPET as a promising, sustainable, and cost-effective PEM derived from plastic waste, with strong potential for practical deployment in VRFB systems.

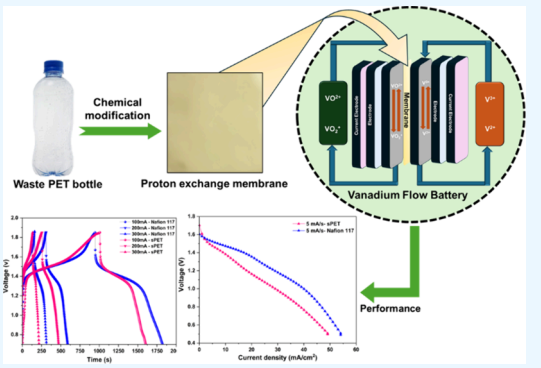

KEYWORDS: *Vanadium redox flow batteries, PET waste bottle, Proton exchange membrane, Sustainable, Electrochemical energy storage*

1. INTRODUCTION

Energy storage systems (ESSs) have become crucial for the sustainability of our civilization and are particularly relevant for the efficient use and integration of renewable energy sources.[1] As the global energy transition accelerates, the ability to store electricity reliably and sustainably is crucial for addressing the intermittency of solar and wind power and ensuring grid stability.[2] Among the various storage technologies,[3,4] vanadium redox flow batteries (VRFBs) have emerged as a promising technology for large-scale energy storage due to their long cycle life, flexible design, excellent reversibility, and the unique ability to decouple energy and power.[5−7] This makes VRFBs especially suitable for stationary storage in a renewable energy system. In contrast to conventional batteries, VRFBs store energy in external liquid electrolyte tanks, allowing for the independent scaling of power, determined by the cell stack, and energy, determined by the electrolyte volume.[8,9] The VRFB uses two vanadium-based electrolytes that circulate and react when they flow inside the cell. The discharge reaction involves the spontaneous oxidation of V^{2+} ions at the negative electrode and reduction of vanadium ions from the oxidation number +5 to +4:

$$V^{2+} \rightarrow V^{3+} + e^{-}$$

$$VO_2^{+} + 2H^{+} + e^{-} \rightarrow VO^{2+} + H_2O$$

The electrolyte is a sulfuric acid solution containing the vanadium ions, and the charge carrier across the cell is the H^{+} ion. The proton exchange membrane (PEM) enables selective proton transport while suppressing vanadium ion crossover between half-cells,[10] playing a critical role in the system's energy efficiency, capacity retention, and long-term operational stability, particularly under the harsh, acidic, and oxidative conditions typical of VRFB operation.[11] The membrane is typically made of Nafion, a polymer derived from perfluorosulfonic acid (PFSA).[12] Nafion has a unique microphase-separated structure, comprising a hydrophobic polytetrafluoroethylene (PTFE) backbone with sulfonated perfluoro(alkyl vinyl ether) side chains, which provide high proton conductivity along with excellent chemical, thermal, and oxidative stability, establishing Nafion as the benchmark PEM for redox flow battery systems.[13,14] Despite its proven advantages, Nafion faces growing concerns regarding its economic and environmental sustainability. Its high production cost of up to US$1733 per square meter poses a significant

Received: October 23, 2025
Revised: January 4, 2026
Accepted: January 4, 2026
Published: February 5, 2026

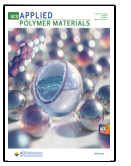

https://doi.org/10.1021/acsapm.5c03977
ACS Appl. Polym. Mater. 2026, 8, 2653−2661

barrier to large-scale deployment in energy storage systems.[13,15] Moreover, its reliance on fluorinated monomers such as tetrafluoroethylene results in toxic byproducts and contributes to the persistence of polyfluoroalkyl substances in the environment. These substances are resistant to degradation and have been detected in ecosystems and living organisms, raising serious health and environmental concerns.[15−17] In response, regulatory agencies, including the European Commission, have proposed restrictions on PFAS use in industrial applications.[18,19] These challenges underscore the urgent need for cost-effective, fluorine-free alternatives to Nafion for next-generation PEM.

In response to the limitations of fluorinated membranes, research has increasingly focused on developing alternatives based on hydrocarbon polymers. A variety of PEMs have been developed for redox flow applications, including sulfonated poly(ether ether ketone) (sPEEK), polybenzimidazole (PBI), sulfonated polyimides, and other hydrocarbon-based sulfonated polymers. Another suitable candidate would be polyethylene terephthalate (PET), a widely used aromatic polyester found in beverage bottles and consumer packaging.[20] PET is globally abundant, mechanically robust, and chemically stable.[21,22] Additionally, PET's unique chemical structure, featuring terephthalic acid (TPA) and ethylene glycol (EG), contains aromatic rings and hydroxyl groups that serve as reactive sites for chemical modification.[23,24] Recent advances in chemical modification techniques, particularly sulfonation, have enabled the upcycling of waste PET into sulfonated PET (sPET) membranes.[15,25] Unlike Nafion, sPET membranes are free of fluorinated compounds, derived from widely available plastic waste, and can be produced at approximately one-third the cost (estimated US$1.56 per 25 cm^2 (≈US$624 m^{-2}), this estimated cost reflects only materials and reagents that consumed in membrane preparation, excluding labor, capital equipment, utilities, and scale-up overheads; therefore, it should be interpreted as an order-of-magnitude comparison rather than a full techno-economic analysis. Therefore, sPET membrane offers a more sustainable and economically viable alternative for future energy storage technologies. The sPET membrane used in this study was previously synthesized via a two-step sulfonation process and thoroughly characterized for PEM fuel cell applications by Neelalochana et al.[15,26] The membrane demonstrated an ion exchange capacity (IEC) of 1.28 ± 0.15 mequiv/g, a water uptake of 6.02 ± 1.30% at 80 °C, and a swelling ratio of 18.25 ± 0.3% in-plane and 26.45 ± 0.4 through plane at 80 °C. The hydration number (λ) was calculated to be 15.62. Additionally, the membrane exhibited a high ionic conductivity, reaching a maximum of 157.3 mS/cm at 80 °C. These properties are essential for evaluating its suitability in redox flow battery operation.

In this study, we evaluated for the first time the viability of novel sPET membranes, derived from waste PET bottles, for VRFB applications. The study uniquely assesses the membranes' performance through single-cell charge−discharge cycling, Potentiodynamic polarization, and electrochemical impedance spectroscopy (EIS), side-by-side comparison with commercial Nafion 117. The obtained results highlight the potential of sPET membranes as fluorine-free alternatives for energy storage applications.

2. EXPERIMENTAL SECTION

2.1. Materials

PET waste bottles were collected from discarded water bottles, and Nafion 117 membranes were obtained from DuPont and used as a benchmark material. All reagents and solvents, including vanadium(V) oxide (V_2O_5, 98%), oxalic acid (99%), sulfuric acid (H_2SO_4, 95−98%), ethylene glycol (99.8%), zinc acetate (99%), 4,4′-diamino-2,2′-stilbenedisulfonic acid (85%), triethylamine (99.8%), benzoic acid (99.8%), m-cresol (99.9%), ethyl acetate (99%), phenolphthalein, 1,1,3,3,3-hexafluoroisopropanol (99%), and ethylene carbonate (98%) were purchased from Sigma-Aldrich.

2.2. Membrane Preparation and Activation: sPET and Nafion 117

Waste PET bottles were chemically modified to the BHET intermediate via glycolysis with ethylene glycol and then reacted with the 4,4′-diamino-2,2′-stilbenedisulfonic acid (DSSA) to synthesize a sulfonated PET-based polymer (sPET). Different degrees of sulfonation for bis(2- hydroxyethyl) terephthalate (BHET): DSSA feed ratios were investigated (e.g., 1:1, 2:1, and 3:1). In this study, the sPET used for membrane fabrication was prepared using a 1:1 molar ratio of BHET to DSSA, corresponding to an estimated degree of sulfonation of 50%.[15] This ratio demonstrated a good balance between the physical and morphological properties of the membrane obtained by the solution casting technique. In this method, basically, sPET powder was dissolved in a suitable amount of 1,1,3,3,3-hexafluoroisopropanol, stirred, and cast in a glass plate. The obtained flexible membrane was kept in distilled water before activation. The chemical modification of waste PET bottles into sPET material and subsequently the PEM preparation have been discussed in detail in our previous work.[15]

Before cell assembly, all membranes underwent a proper activation process to ensure optimal ionic conductivity and removal of any surface contaminants.[27] The sPET membrane was activated by soaking in a 1 M H_2SO_4 solution for 1 h. For the Nafion 117 membrane, first, it was immersed in 30% H_2O_2 at 80 °C for 30 min to eliminate organic contaminants and activate the surface, followed by boiling in distilled water for 30 min to remove residual oxidants. Subsequently, the membranes were soaked in 0.5 M H_2SO_4 at 80 °C for 30 min and finally boiled again in distilled water for 30 min to ensure complete protonation and hydration.

2.3. Electrolyte Preparation

The vanadium electrolyte was prepared by dissolving vanadium pentoxide (V_2O_5) in deionized (DI) water acidulated with 6 M H_2SO_4. The solution was heated to approximately 200 °C under continuous stirring to ensure complete dissolution of 44.56 g of V_2O_5 to obtain 0.5 M VO_2^+ ions.

To obtain vanadium(IV) (VO^{2+}), a chemical reduction step was performed using oxalic acid as the reducing agent. The reduction reaction 1 follows the stoichiometry:

$$2VO_2^+ + C_2O_4^{2-} + 4H^+ \rightarrow 2VO^{2+} + 2CO_2 + 2H_2O \quad (1)$$

Here, one mole of oxalic acid reduces two moles of VO_2^+. In this process, two 250 mL borosilicate glass electrolyte reservoirs of VO_2^+ solution were treated with 0.125 mol (15.92 g) of oxalic acid and heated to 60−70 °C until the evolution of CO_2 gas ceased, indicating the completion of the reaction. Following this, the vanadium redox flow battery cell was assembled using the VO^{2+} ion in both electrolytes, and an initial electrochemical charging step was carried out. During this process, the V(IV) ion was oxidized back to the V(V) state at the anode, while V^{3+} was produced at the cathode. Subsequently, the portion of VO_2^+ in the positive electrolyte was chemically reduced once again using oxalic acid, following the same procedure as before. To achieve the fully reduced and balanced electrolyte configuration required for VRFB operation, the V(V) electrolyte was again chemically reduced to the 4+ state before a second charging step was applied. This converted the negative electrolyte to V^{2+} and regenerated VO_2^+ on the positive side, resulting

https://doi.org/10.1021/acsapm.5c03977
ACS Appl. Polym. Mater. 2026, 8, 2653−2661

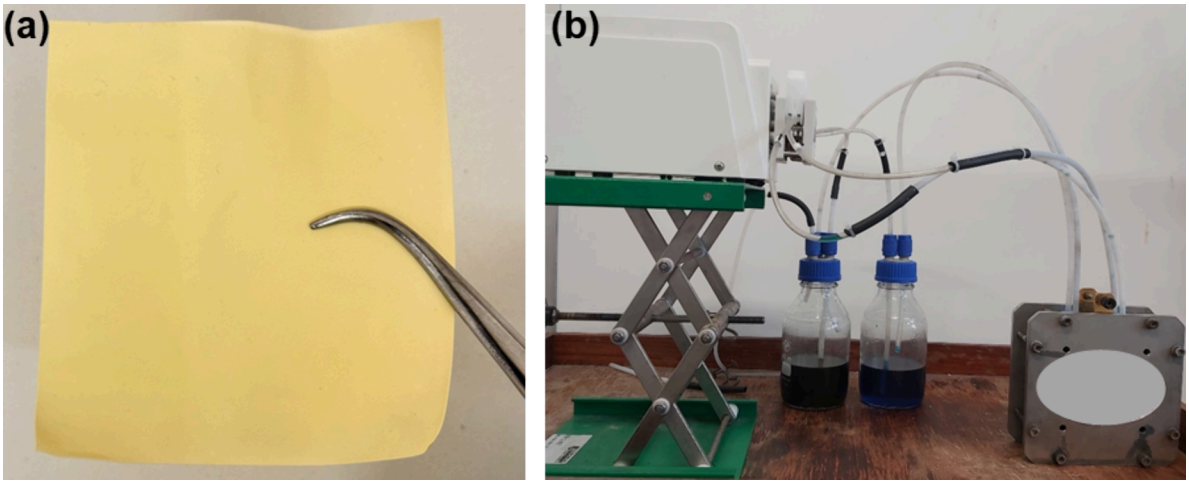

Figure 1. (a) Physical morphology of the sPET membrane, and (b) Experimental setup of the VRFB, showing the peristaltic pump (left), two 250 mL electrolyte reservoirs (positive and negative, total volume 500 mL) (center), and the flow cell (right).

in the final configuration of 250 mL of V^{2+} on the negative side and 250 mL of VO_2^+ on the positive side. This completed the preparation process and ensured the cell was ready for VRFB testing.

2.4. Cell Setup

The cell was a commercially available module,[28] with an active area of 25 cm^2. Gold-plated copper current collectors were mounted on both end plates, with interdigitated graphite flow fields, carbon paper electrodes, and the test membrane being assembled in the following sequence, starting from the membrane: gasket | carbon paper | flow field on graphite end plate | current collector. The description of the scheme can be found elsewhere.[29] A uniform compression was applied by diagonally cross-tightening bolts to a torque of 6 N·m to ensure proper sealing and contact. The cell was connected to two 500 mL borosilicate glass electrolyte reservoirs via PTFE tubing. Electrolyte circulation was maintained using a peristaltic pump (Longer L100-1S-2), operating at a constant flow rate. The positive reservoir was equipped with two ports, while the negative reservoir included a third port to enable nitrogen purging, preventing oxidation of V^{2+} by air during operation. Silicone tubing was used within the pump head and connected in series with PTFE lines to ensure stable, pulsation-free flow through the cell. The membrane (average thickness 60 μm) and the complete VRFB test setup are shown in Figure 1(a) and (b). Details of the pump calibration and flow control setup are provided in the Supporting Information (Section S1).

2.5. Characterization

All electrochemical measurements, including charge−discharge cycling, polarization curve acquisition, and EIS measurements, were performed using a Gamry Interface 5000E potentiostat (Gamry Instruments, USA) with a sinusoidal perturbation amplitude of 10 mV (rms) around the selected operating point. The frequency range was 10 μHz to 1 MHz. (Instrument limits: maximum applied potential 6 V; maximum current range 5 A.) making it particularly suitable for high-precision testing of energy storage and conversion devices. All VRFB tests in this study were performed at room temperature to provide a controlled baseline for an initial demonstration and a direct, side-by-side comparison between sPET and Nafion 117. In practical operation, temperature is expected to enhance proton conductivity due to faster ion transport and increased polymer mobility, but it may also increase vanadium crossover by increasing diffusion coefficients and by altering membrane hydration/swelling, which could reduce Coulombic efficiency. Elevated temperature can further accelerate chemical and mechanical degradation processes in strongly acidic vanadium electrolytes over extended operation.

The mechanical behavior of the sPET membrane was evaluated using a custom-built tensile test setup. This setup comprises a motor-driven actuator, a load-sensing spring, and silicon sheet grips, with images of the membranes captured during a tensile test via an optical microscope, as previously reported.[30] The sPET membrane samples were cut into rectangular strips with an average gauge length of 2.6 mm and average width of 2.3 mm, and then carefully glued onto the testing apparatus before measurement (Figure 7(a) and (b)). The mechanical properties, such as strength, Young's modulus, and failure strain, were derived from the stress−strain curves.[31] Membranes were tested under two different conditions: (a) wet and (b) dry. All tests were performed at room temperature.

3. RESULTS AND DISCUSSION

3.1. Polarization Curves

The polarization behavior of VRFBs assembled with s-PET and Nafion 117 membranes under stagnant conditions was evaluated at scan rates of 1, 3, and 5 mA/s, as illustrated in Figure 2. All polarization curves exhibited the typical three-stage profile: an activation-controlled region at low current densities, a linear ohmic region at intermediate current densities, and a mass transport-limited region at higher currents. At low scan rates (1 mA/s), both membranes exhibited sharper voltage drops, indicating sluggish kinetics and a stronger influence of charge transfer and ion transport

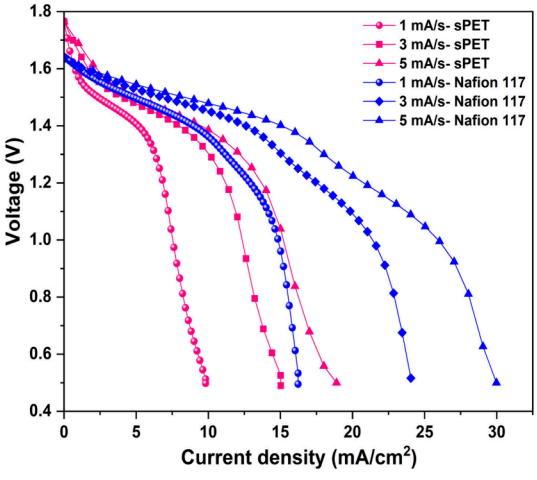

Figure 2. Polarization curves of VRFBs assembled with Nafion 117 and sPET membranes under stagnant mode, recorded at scan rates of 1, 3, and 5 mA/s using a 0.5 M vanadium.

https://doi.org/10.1021/acsapm.5c03977
ACS Appl. Polym. Mater. 2026, 8, 2653−2661

resistances. As the scan rate increased to 5 mA/s, the ohmic region became more distinctly defined, and the transition to the diffusion-limited regime was delayed. This shift suggests that at higher scan rates, the impact of concentration gradients is reduced due to shorter reaction times, thereby improving the apparent transport characteristics and delaying mass transport limitations. Across all scan rates, the sPET membrane displayed a more pronounced voltage decline, particularly in the ohmic and diffusion-controlled regions, reflecting its relatively lower ion conductivity and potentially thicker membrane morphology. Despite its moderate performance under stagnant conditions, the improved definition of the ohmic region at higher scan rates for sPET indicates that its electrochemical behavior is significantly affected by operational parameters. In contrast, Nafion 117 consistently exhibited higher cell voltages and broader current density ranges attributed to its lower internal resistance. These observations support the potential viability of the sPET membrane under optimized or dynamic flow conditions.

However, under electrolyte circulation conditions (Figure 3), both membranes exhibited comparable open-circuit

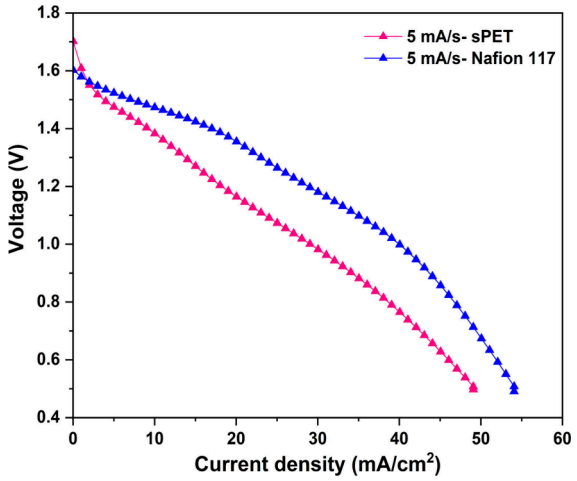

Figure 3. Polarization curves of VRFBs assembled with Nafion 117 and sPET membranes under circulation mode at a scan rate of 5 mA/s using 0.5 M vanadium.

voltages (OCVs) of approximately 1.60 V, confirming effective ionic selectivity and minimal self-discharge. The polarization curves recorded at a scan rate of 5 mA/s showed significant performance improvement compared to stagnant operation, reflecting the benefits of forced electrolyte flow in reducing concentration polarization and enhancing mass transport. In this dynamic regime, the voltage drops across the entire current density range were less steep for both membranes. Notably, the sPET membrane, although showing lower overall voltages and a reduced maximum current density (47 mA cm^{-2}), exhibited a smoother voltage profile and diminished mass transport limitations under flow conditions compared to stagnant operation. In comparison, Nafion 117 consistently maintains higher cell voltages and reaches a maximum current density of 55 mA cm^{-2}. This superior performance is attributed to its higher proton conductivity. To fully assess practical viability, long-term charge−discharge cycling under fixed current loads was performed to evaluate electrochemical durability.

3.2. Charge−Discharge Cycles

The charge−discharge characteristics of VRFB incorporating each of the membranes were evaluated as shown in Figure 4.

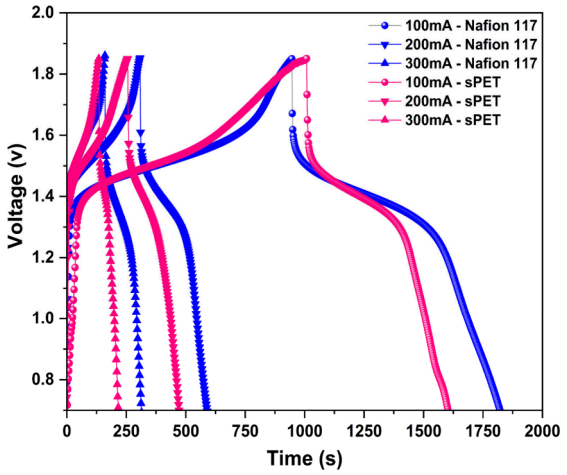

Figure 4. Charge−discharge curves of VRFBs using Nafion 117 and sPET membranes at constant current densities of 100, 200, and 300 mA cm^{-2} in 0.5 M vanadium.

At all tested currents, the cells exhibited well-defined charge plateaus near 1.8−1.9 V and discharge plateaus around 1.4−1.6 V, characteristic of the V(IV)/V(V) and V(II)/V(III) redox couples.[32] At 100 mA cm^{-2}, both membrane systems displayed similar charge−discharge profiles and stable cycling behavior, with minimal voltage losses. However, as the current increased to 200 and 300 mA cm^{-2}, a progressive increase in voltage polarization was observed, particularly for the sPET membrane. The sPET membrane showed a steeper voltage decline during discharge at 300 mA cm^{-2}, suggesting higher ohmic and mass transport limitations under elevated current stress. Despite this, the sPET membrane maintained reasonably stable behavior at moderate currents (up to 200 mA), indicating its viability for low-to-medium power VRFB operations.[6] In contrast, Nafion 117 consistently achieved longer discharge durations in the range of 20−25% for the three current densities and higher Coulombic efficiency (66−80%) across all current loads, reflecting its lower internal resistance and more efficient ion transport.[33] These findings underscore the consistent electrochemical performance of Nafion 117, particularly under elevated current loads. Nonetheless, the relatively stable performance of the sPET membrane at moderate current densities is valuable. The obtained results demonstrate the initial proof of concept (rather than long-term stability) using a cost-effective sPET membrane alternative to commercial Nafion, provided that operational parameters are properly optimized to mitigate performance losses at higher loads.

3.3. EIS Analysis

EIS was employed to investigate the internal resistances and charge transfer behavior of sPET and Nafion 117 membranes in VRFBs under circulating and static electrolyte conditions, as shown in Figure 5(a) and (b), respectively. Measurements were performed over a frequency range of 50.000 to 0.01 Hz with 7 points per decade, ensuring adequate resolution across all relevant electrochemical processes. Under electrolyte circulation (Figure 5(a)), both systems exhibited typical Nyquist profiles characterized by a high-frequency intercept

https://doi.org/10.1021/acsapm.5c03977
ACS Appl. Polym. Mater. 2026, 8, 2653−2661

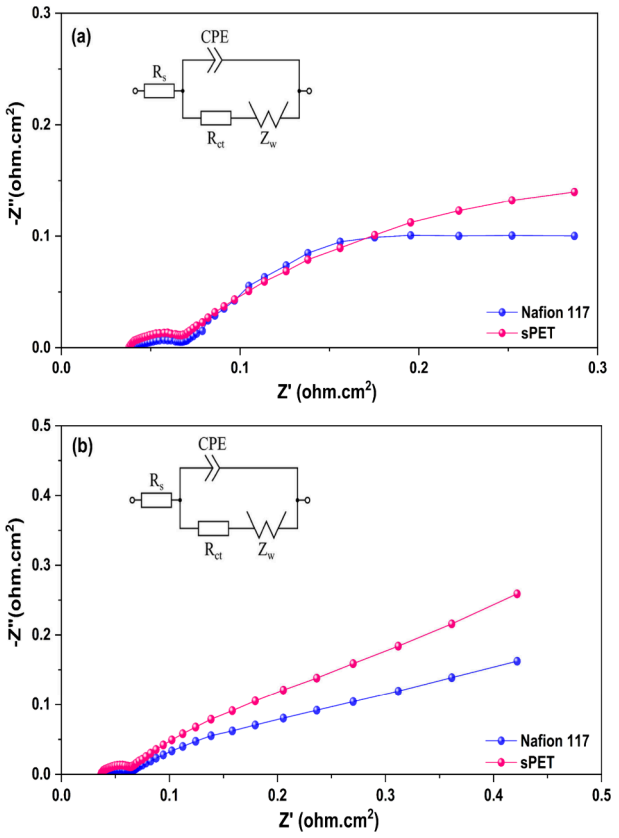

Figure 5. (a) Nyquist plots of VRFBs with Nafion 117 and sPET membranes under electrolyte circulation (flow rate 20 mL min^{-1}), and (b) Nyquist plots under stagnant conditions. Electrolyte: 0.5 M vanadium.

(bulk ohmic resistance, R_Ω), which is predominantly attributed to the membrane's resistance to ionic (proton) flow; a depressed semicircle (charge transfer resistance, R_{ct}),[34,35] and a low-frequency Warburg tail (diffusion resistance).[36−39] Overall, the sPET membrane shows good impedance behavior under electrolyte circulation, with values closely approaching those of Nafion 117, which remains slightly lower due to its higher intrinsic proton conductivity. These results reinforce the promise of sPET membranes as cost-effective, fluorine-free alternatives in redox flow battery systems. The thickness of the membranes also directly influences ohmic resistance and overall cell performance. In our study, the sPET membrane had a thickness of 60 μm, while Nafion 117, used as the benchmark, has a nominal thickness of 183 μm. The reduced thickness of sPET contributes to lower area-specific resistance and improved ionic transport, though it may also enhance vanadium crossover to some extent, particularly at low current densities. In contrast, the greater thickness of Nafion 117 inherently suppresses vanadium crossover and supports higher CE; however, this added thickness can be partly compensated by Nafion's higher proton conductivity, which can impact VE at higher current densities.

The observed resistive characteristics, particularly Rct and RΩ, play a critical role in determining the energy efficiency of the system, which is discussed in the following section. Nafion 117 exhibited a slightly lower R_{ct} (30 mΩ) compared to sPET (31 mΩ), suggesting marginally better interfacial charge transfer, attributable to its higher proton conductivity and optimized morphology. However, the difference is minimal, and sPET shows comparable impedance behavior under dynamic conditions, supporting its viability as a functional PEM in practical VRFB setups. In stagnant conditions (Figure 5(b)), total impedance increased for both membranes, reflecting the expected suppression of convective transport and more pronounced concentration polarization. The R_{ct} values decreased to 27 mΩ (Nafion 117) and 29 mΩ (sPET), likely due to ion redistribution at the membrane-electrode interface. Nevertheless, sPET exhibited a more extended diffusion tail, suggesting greater susceptibility to diffusion limitations in the absence of flow, a behavior consistent with the polarization and charge−discharge results.[40] Overall, while Nafion 117 maintains a slight advantage, sPET performs comparably in terms of impedance, especially under circulation. The impedance findings, particularly regarding charge transfer and ohmic resistances, directly impact the overall energy efficiency of the VRFB system. These effects are quantified through the following efficiency analysis.

3.4. Cell Efficiencies

The Coulombic efficiency (CE), voltage efficiency (VE), and energy efficiency (EE) of VRFBs assembled with sPET and Nafion 117 membranes were evaluated at constant current loads of 100, 200, and 300 mA cm^{-2} using 0.5 M vanadium (Figure 6). CE reflects the balance between useful charge and

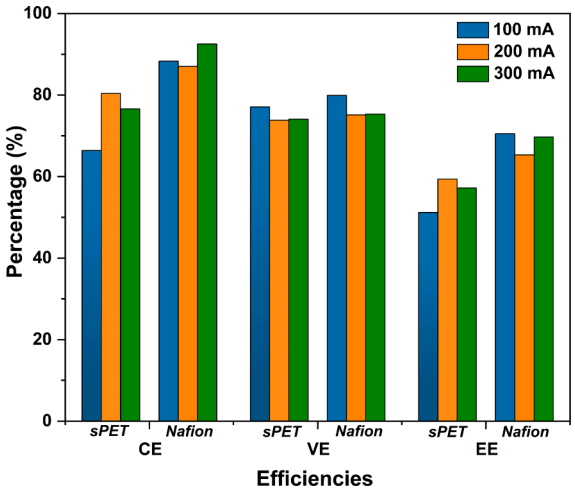

Figure 6. Comparison of CE, VE, and EE of VRFBs using sPET and Nafion 117 membranes at three different current densities (100, 200, and 300 mA cm^{-2}) in 0.5 M vanadium.

parasitic losses from vanadium crossover/self-discharge. Increasing the current density from 100 to 200 mA cm^{-2} shortens the cycle time (which tends to reduce total crossover). Still, it also steepens concentration/Donnan gradients and increases electro-osmotic drag during charge, transiently raising crossover flux. Under our fixed flow and volume conditions, this stronger driving force at 200 mA cm^{-2} slightly outweighed the shorter cycle time, yielding a modestly lower CE than at 100 mA cm^{-2} for Nafion; the difference lies within the error bars from replicate runs.

The sPET membrane exhibited promising and improving performance, especially considering its early stage development. While the CE of sPET was initially lower (66.4% at 100 mA cm^{-2}), it improved markedly at higher current (80.4% at 200 mA cm^{-2}), highlighting the reduced influence of vanadium crossover at higher current operation. As a result, Coulombic

https://doi.org/10.1021/acsapm.5c03977
ACS Appl. Polym. Mater. 2026, 8, 2653−2661

Table 1. Comparison of sPET and Representative Nonfluorinated Membranes for Vanadium Redox Flow Batteries

Membrane (polymer)	Thickness (μm)	Test current (mA cm^{-2})	CE (%)	VE (%)	EE (%)	Ref
SPES 50/50(hydrocarbon block copolymer)	53	20	97.6 ± 0.1	72.8 ± 0.2	71.0 ± 0.2	41
SPEEK/FCB-3 (hydrocarbon composite)	62	120	99.49	–	83.46	42
SPEEK–ZrO_2 (SP–Z-5, hydrocarbon composite)	70	200	99.01	81.95	81.11	43
SPEEK/g-C_3N_4-1.5	79–81	30	97.5	–	83.6	44
S/DCNTs-HPW-1	–	50 → 160	98.2 → 99.4	91.2 → 69.4	89.5 → 69.0	45
Nafion 117	183	100 → 300	87.0–92.5	75.1–79.9	65–70	(this work)
sPET	60	100 → 200	66.4 → 80.4	~77.1 (at 100)	51–59	(this work)

losses become less significant. In contrast, Nafion 117 delivers higher overall efficiencies across all current densities, with CE values ranging from 87.0% to 92.5% and VE from 79.9% to 75.1%, reflecting its optimized structure, high ionic conductivity, and inherently lower vanadium permeability. The relatively lower CE of sPET at low currents can be attributed to incomplete suppression of vanadium ion crossover, which is influenced by both the sulfonation degree and the dense but not fully optimized morphology of the PET matrix. Nevertheless, the observed improvement with current density highlights sPET's potential adaptability to operating conditions, an encouraging trait for practical VRFB applications.

Voltage efficiency also followed a gradual decline with increasing current for both membranes due to increased overpotentials and ohmic losses. While Nafion maintained slightly higher VE values overall, the performance gap with sPET was relatively small (e.g., 77.1% vs 79.9% at 100 mA cm^{-2}), indicating that the electrical resistance of sPET is already within a competitive range. As a result, the energy efficiency of sPET ranged from 51% to 59%, compared to 65–70% for Nafion. Although Nafion leads in total efficiency, the performance trajectory of sPET, particularly at intermediate currents, highlights its viability as a cost-effective and sustainable membrane solution, especially with further optimization of the polymer structure and functionalization. Table 1 presents a comparison of the sPET membrane with representative nonfluorinated PEMs reported for VRFBs, contextualizing our CE/VE/EE at comparable thicknesses and current densities while also highlighting remaining gaps in low-current CE and vanadium selectivity.

3.5. Mechanical Characterization

Mechanical robustness is crucial for the long-term durability of membranes under various mechanical loading and boundary conditions in VRFBs. Figure 7(c) shows the stress–strain curves corresponding to the wet (Figure 7(a)) and dry (Figure 7(b)) sPET membrane. The dry membrane demonstrated significantly higher tensile strength (7.9 ± 0.9 MPa) and elastic modulus (683 ± 32 MPa) than the wet membrane (4.2 ± 0.1 MPa and 155 ± 32 MPa, respectively), indicating that the dry polymer network possesses greater structural stiffness and rigidity due to strong polymer–polymer interactions such as hydrogen bonding and van der Waals forces.[46] In contrast, the wet sPET membrane exhibited higher stretchability, as reflected by its higher elongation at break (21 ± 2%) compared to the dry one (5.5 ± 1.6%). This behavior is attributed to the presence of water molecules, which disrupt interchain interactions by forming hydrogen bonds with sulfonic acid groups, thereby increasing chain mobility and softening the polymer network, a phenomenon commonly referred to as plasticization.[47] Our previous study[15] showed that the water uptake of the sPET membrane was relatively low

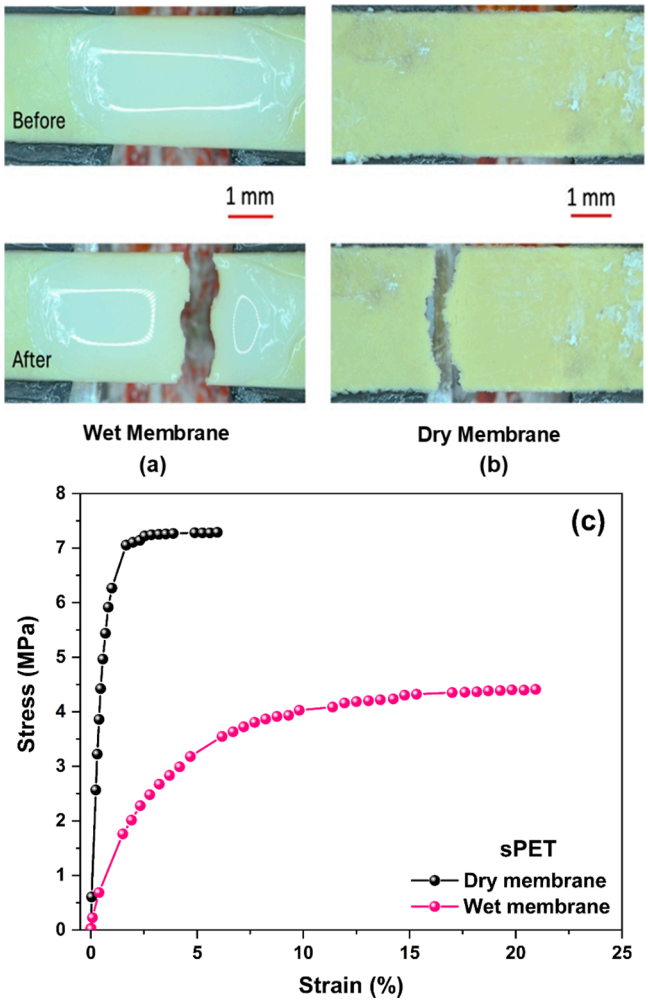

Figure 7. Mechanical characterization of sPET MEM: Optical image of (a) wet membrane, (b) dry membrane, and (c) the representative stress–strain curves as determined by uniaxial tensile tests.

(~16.2% at 20 °C), which limits the degree of plasticization. As a result, the polymer chains remain less flexible, leading to a stiffer membrane with reduced elongation at break and a higher elastic modulus[48] under dry conditions. Figure S2 displays the stress–strain curves corresponding to the sPET membranes under both wet and dry conditions.

For comparison, literature data indicate that a dry Nafion membrane (thickness: 50.8 mm) exhibits a tensile strength of approximately 21.2 MPa, a Young's modulus of around 197.2 MPa, and an elongation at break of about 155.2%.[49] These results indicate that Nafion maintains a balance of tensile strength and ductility, whereas sPET is significantly stiffer but less extensible in the dry state. This difference is consistent

https://doi.org/10.1021/acsapm.5c03977
ACS Appl. Polym. Mater. 2026, 8, 2653–2661

with stronger interchain interactions in sPET and greater chain mobility in Nafion. These values of Nafion's favorable balance between mechanical strength and flexibility. While the sPET membrane displays lower tensile strength and elongation, it exhibits significantly higher stiffness in its dry state. This mechanical behavior can be further explained by the underlying chemical structure of the sPET membrane, which features a rigid aromatic backbone with sulfonic acid groups directly attached to the benzene rings via short linkers. This compact architecture promotes strong interchain interactions (hydrogen bonding and $\pi-\pi$ stacking), resulting in increased stiffness but limited flexibility. Additional discussion of structure−property relationships of Nafion is provided in the Supporting Information (Section S2). To improve the mechanical properties of sPET, particularly under hydrated conditions, strategies such as polymer cross-linking, incorporation of flexible linkers, or nanocomposite reinforcement may be employed to enhance stretchability without compromising strength.[50]

4. CONCLUSION

This work is intended as an initial demonstration of the potential of sulfonated PET (sPET) membranes, derived from waste PET bottles, as sustainable alternatives for vanadium redox flow battery (VRFB) applications. The sPET membrane showed only a slightly higher internal resistance than Nafion. Charge−discharge cycling confirmed stable performance at moderate current densities, while EIS revealed nearly equivalent charge transfer resistance values of approximately 31 mΩ for both sPET and Nafion membranes under electrolyte circulation. Even under stagnant conditions, the sPET membrane maintained acceptable transport properties. Despite Nafion's established benchmark performance, the sPET membrane delivered competitive Coulombic efficiencies (66−80%) and energy efficiencies (51−59%), particularly under optimized flow conditions.

However, we should also take into account that the hydrocarbon-based PEMs can be challenged by oxidative chemical environments, particularly at high state-of-charge, where vanadium(V) species (primarily VO_2^+ in the positive electrolyte) and associated radical-mediated pathways may promote polymer oxidation. In the case of sulfonated PET, additional sensitivity may arise from the presence of ester linkages that can undergo hydrolysis under strongly acidic conditions, potentially leading to chain scission and gradual loss of mechanical integrity over extended operation. To mitigate these effects, several practical strategies could be explored: (i) controlled cross-linking or network formation to suppress swelling and enhance mechanical retention; (ii) incorporation of functionalized nano fillers that have double functionalities as they can improve both physical and chemical stabilities; and (iii) further tuning of sulfonation level and membrane morphology to balance proton conductivity against ion permeability. These directions are the focus of ongoing work to translate the promising initial VRFB performance of sPET toward long-term, durable operation. Overall, the obtained experimental evidence underscores not only the electrochemical viability of upcycled sPET in VRFB systems but also, by transforming waste PET bottles into high-performance and mechanically stable PEM, this work provides a compelling pathway toward environmentally responsible, fluorine-free PEMs for energy storage solutions.

■ ASSOCIATED CONTENT

Supporting Information

The Supporting Information is available free of charge at https://pubs.acs.org/doi/10.1021/acsapm.5c03977.

Figure S1: Flow rate calibration and pump setup. Figure S2: Mechanical characterization. (PDF)

■ AUTHOR INFORMATION

Corresponding Author

Narges Ataollahi − *Department of Civil, Environmental & Mechanical Engineering, University of Trento, 38123 Trento, Italy*; orcid.org/0000-0002-8135-6054; Email: narges.ataollahi@unitn.it

Authors

Marco Morelli − *Department of Civil, Environmental & Mechanical Engineering, University of Trento, 38123 Trento, Italy*

Varun Donnakatte Neelalochana − *Department of Civil, Environmental & Mechanical Engineering, University of Trento, 38123 Trento, Italy*

Vivek Manish − *Department of Civil, Environmental & Mechanical Engineering, University of Trento, 38123 Trento, Italy*

Alda MP Simões − *Centro de Química Estrutural, Institute of Molecular Sciences, Departamento de Engenharia Química, Instituto Superior Técnico, 1049-001 Lisboa, Portugal*

Maria F. Pantano − *Department of Civil, Environmental & Mechanical Engineering, University of Trento, 38123 Trento, Italy*; orcid.org/0000-0001-5415-920X

Paolo Scardi − *Department of Civil, Environmental & Mechanical Engineering, University of Trento, 38123 Trento, Italy*; orcid.org/0000-0003-1097-3917

Complete contact information is available at: https://pubs.acs.org/10.1021/acsapm.5c03977

Author Contributions

[§]Marco Morelli and Varun Donnakatte Neelalochana contributed equally to this work.

Notes

The authors declare no competing financial interest.

■ ACKNOWLEDGMENTS

The authors gratefully acknowledge the Programma Operativo Nazionale (PON) 2014−2020 on Innovation and Green for supporting this research activity. The sixth and last authors acknowledge the Italian Ministry of Universities and Research (MUR) for funding this work through the DICAM EXC project (Departments of Excellence 2023−2027, grant L232/2016).

■ REFERENCES

(1) Worku, M. Y. Recent Advances in Energy Storage Systems for Renewable Source Grid Integration: A Comprehensive Review. *Sustainability.* **2022**, *14* (10), 5985.

(2) Elalfy, D. A.; Gouda, E.; Kotb, M. F.; Bureš, V.; Sedhom, B. E. Comprehensive Review of Energy Storage Systems Technologies, Objectives, Challenges, and Future Trends. *Energy Strateg. Rev.* **2024**, *54*, 101482.

(3) Azaki, N. J.; Ahmad, A.; Hassan, N. H.; Mohd Abdah, M. A. A.; Su'ait, M. S.; Ataollahi, N.; Lee, T. K. Poly(Methyl Methacrylate)

Grafted Natural Rubber Binder for Anodes in Lithium-Ion Battery Applications. *ACS Appl. Polym. Mater.* **2023**, *5* (7), 4953−4965.
(4) Energy Storage Grand Challenge, Energy Storage Market Report, **2020**. *U.S. Department of Energy*. https://www.energy.gov/energy-storage-grand-challenge.
(5) Wang, H.; Pourmousavi, S. A.; Soong, W. L.; Zhang, X.; Ertugrul, N. Battery and Energy Management System for Vanadium Redox Flow Battery: A Critical Review and Recommendations. *J. Energy Storage.* **2023**, *58*, 106384.
(6) Sharmoukh, W. Redox Flow Batteries as Energy Storage Systems: Materials, Viability, and Industrial Applications. *RSC Adv.* **2025**, *15* (13), 10106−10143.
(7) Shi, N.; Wang, G.; Wang, Q.; Wang, L.; Li, Q.; Yang, J. Acid Doped Branched Poly(Biphenyl Pyridine) Membranes for High Temperature Proton Exchange Membrane Fuel Cells and Vanadium Redox Flow Batteries. *Chem. Eng. J.* **2024**, *489*, 151121.
(8) Puleston, T.; Clemente, A.; Costa-Castelló, R.; Serra, M. Modelling and Estimation of Vanadium Redox Flow Batteries: A Review. *Batteries.* **2022**, *8* (9), 121.
(9) Wang, Q.; Zhang, Z.; Lv, P.; Peng, Z.; Yang, J. Poly(Terphenyl Pyridine) Based Amphoteric and Anion Exchange Membranes with High Ionic Selectivity for Vanadium Redox Flow Batteries. *Chem. Eng. J.* **2025**, *505*, 158922.
(10) Zhang, Y.; Wang, H.; Liu, B.; Shi, J.; Zhang, J.; Shi, H. An Ultra-High Ion Selective Hybrid Proton Exchange Membrane Incorporated with Zwitterion-Decorated Graphene Oxide for Vanadium Redox Flow Batteries. *J. Mater. Chem. A* **2019**, *7* (20), 12669−12680.
(11) Yuan, X. Z.; Song, C.; Platt, A.; Zhao, N.; Wang, H.; Li, H.; Fatih, K.; Jang, D. A Review of All-Vanadium Redox Flow Battery Durability: Degradation Mechanisms and Mitigation Strategies. *Int. J. Energy Res.* **2019**, *43* (13), 6599−6638.
(12) Brahma, K.; Nayak, R.; Verma, S. K.; Sonika. Recent Advances in Development and Application of Polymer Nanocomposite Ion Exchange Membrane for High-Performance Vanadium Redox Flow Battery. *J. Energy Storage.* **2024**, *97*, 112850.
(13) Sharma, A.; Đelević, L.; Herkendell, K. Next-Generation Proton-Exchange Membranes in Microbial Fuel Cells: Overcoming Nafion's Limitations. *Energy Technol.* **2024**, *12* (6), 1−26.
(14) Niccolai, F.; Guazzelli, E.; Cesari, A.; El Koura, Z.; Pucher, I.; Galli, G.; Martinelli, E. Sulfonated Styrene-Grafted Polyvinylidene Fluoride Copolymers for Proton Exchange Membranes for AQDS/Bromine Redox Flow Batteries. *Macromol. Rapid Commun.* **2025**, *46*, 2400852.
(15) Donnakatte Neelalochana, V.; Mancini, I.; Loi, N.; Cufalo, G.; D'Anzi, A.; Scardi, P.; Ataollahi, N. Sustainable Conversion of PET Waste Bottle into Proton Exchange Membranes for Fuel Cells. *ACS Appl. Energy Mater.* **2025**, *8*, 3145−3153.
(16) Zheng, W.; Wang, L.; Deng, F.; Giles, S. A.; Prasad, A. K.; Advani, S. G.; Yan, Y.; Vlachos, D. G. Durable and Self-Hydrating Tungsten Carbide-Based Composite Polymer Electrolyte Membrane Fuel Cells. *Nat. Commun.* **2017**, *8* (1), 1−7.
(17) Thuc, V. D.; Kim, D. Ultra-Thin, Mechanically Durable Reinforced Sulfonated Poly(Fluorenyl Biphenyl) Indole Proton Exchange Membrane for Fuel Cell. *J. Membr. Sci.* **2024**, *694*, 122393.
(18) Santoro, C.; Lavacchi, A.; Mustarelli, P.; Di Noto, V.; Elbaz, L.; Dekel, D. R.; Jaouen, F. What Is Next in Anion-Exchange Membrane Water Electrolyzers? Bottlenecks, Benefits, and Future. *ChemSusChem.* **2022**, *15* (8), No. e202200027.
(19) Cousins, I. T.; Goldenman, G.; Herzke, D.; Lohmann, R.; Miller, M.; Ng, C. A.; Patton, S.; Scheringer, M.; Trier, X.; Vierke, L.; Wang, Z.; Dewitt, J. C. The Concept of Essential Use for Determining When Uses of PFASs Can Be Phased Out. *Environ. Sci. Process. Impacts.* **2019**, *21* (11), 1803−1815.
(20) Sarda, P.; Hanan, J. C.; Lawrence, J. G.; Allahkarami, M. Sustainability Performance of Polyethylene Terephthalate, Clarifying Challenges and Opportunities. *J. Polym. Sci.* **2022**, *60* (1), 7−31.
(21) Wei, H.-S.; Liu, K.-T.; Chang, Y.-C.; Chan, C.-H.; Lee, C.-C.; Kuo, C.-C. Superior Mechanical Properties of Hybrid Organic-Inorganic Superhydrophilic Thin Film on Plastic Substrate. *Surf. Coat. Technol.* **2017**, *320*, 377−382.
(22) Neelalochana, V. D.; Scardi, P.; Ataollahi, N. Polyethylene Terephthalate (PET) Waste in Electrochemical Applications. *J. Environ. Chem. Eng.* **2025**, *13* (3), 116823.
(23) Donnakatte Neelalochana, V.; Tomasino, E.; Di Maggio, R.; Cotini, O.; Scardi, P.; Mammi, S.; Ataollahi, N. Anion Exchange Membranes Based on Chemical Modification of Recycled PET Bottles. *ACS Appl. Polym. Mater.* **2023**, *5* (9), 7548−7561.
(24) Neelalochana, V. D.; Tomasino, E.; Malagutti, M. A.; Mancini, I.; Chiappini, A.; Shadakshari, S.; Terban, M. W.; Hinrichsen, B.; Scardi, P.; Ataollahi, N. Impact of Functionalized Titanium Oxide on Anion Exchange Membranes Derived from Chemically Modified PET Bottles. *Electrochim. Acta* **2024**, *507*, 145170.
(25) Kirshanov, K.; Toms, R.; Aliev, G.; Naumova, A.; Melnikov, P.; Gervald, A. Recent Developments and Perspectives of Recycled Poly(Ethylene Terephthalate)-Based Membranes: A Review. *Membranes.* **2022**, *12* (11), 1105.
(26) Donnakatte Neelalochana, V. *Development of Ion Exchange Membranes for Electrochemical Applications Using PET Waste Bottles*. Ph.D. Thesis, Universita degli Studi di Trento, **2025**. https://hdl.handle.net/20.500.14242/212606.
(27) Pujiastuti, S.; Onggo, H. Effect of Various Concentrations of Sulfuric Acid for Nafion Membrane Activation on the Performance of Fuel Cell. *AIP Conference Proceedings* **2016**, *1711*, 060006.
(28) A-Cell - Electrolyser Test Cell Overview & Assembly Manual, **2024**. *Redox Flow*, https://redox-flow.com.
(29) Kim, K. J.; Park, M. S.; Kim, Y. J.; Kim, J. H.; Dou, S. X.; Skyllas-Kazacos, M. A Technology Review of Electrodes and Reaction Mechanisms in Vanadium Redox Flow Batteries. *J. Mater. Chem. A* **2015**, *3* (33), 16913−16933.
(30) Missale, E.; Maniglio, D.; Speranza, G.; Frasconi, M.; Pantano, M. F. Cellulose Nanocrystal Composites with Enhanced Mechanical Properties for Robust Transparent Thin Films. *ACS Appl. Nano Mater.* **2024**, *7* (16), 18167−18176.
(31) Manish, V.; Arockiarajan, A.; Tamadapu, G. Influence of Water Content on the Mechanical Behavior of Gelatin-Based Hydrogels: Synthesis, Characterization, and Modeling. *Int. J. Solids Struct.* **2021**, *233*, 111219.
(32) Roznyatovskaya, N.; Noack, J.; Fühl, M.; Pinkwart, K.; Tübke, J. Towards an All-Vanadium Redox-Flow Battery Electrolyte: Electrooxidation of V(III) in V(IV)/V(III) Redox Couple. *Electrochim. Acta* **2016**, *211*, 926−932.
(33) Jiang, B.; Yu, L.; Wu, L.; Mu, D.; Liu, L.; Xi, J.; Qiu, X. Insights into the Impact of the Nafion Membrane Pretreatment Process on Vanadium Flow Battery Performance. *ACS Appl. Mater. Interfaces* **2016**, *8* (19), 12228−12238.
(34) Ravikumar, S. B.; Mallu, T. A.; Subbareddy, S.; Shivamurthy, S. A.; Neelalochana, V. D.; Shantakumar, K. C.; Rajabathar, J. R.; Ataollahi, N.; Shadakshari, S. An Enhanced Non-Enzymatic Electrochemical Sensor Based on the Bi_2S_3−TiO_2 Nanocomposite with HNTs for the Individual and Simultaneous Detection of 4-Nitrophenol and Nitrofurantoin in Environmental Samples. *J. Mater. Chem. B* **2024**, *12*, 9005−9017.
(35) Subbareddy, S.; Arehalli Shivamurthy, S.; Basavapura Ravikumar, S.; Mylnahalli Krishnegowda, H.; Shadakshari, S.; Selvaraj, M.; Basumatary, S. Structural Crystal Engineering for Energy: Unleashing the Potential of Metal-Organic Frameworks for Photocatalytic Reduction of Carbon Dioxide. *Mater. Today Chem.* **2024**, *40*, 102197.
(36) Uygun, H. D. E.; Uygun, Z. O. Electrochemical Impedance Spectroscopy (EIS) Principles and Biosensing Applications. *Handb. Nanobioelectrochemistry Appl. Devices Biomol. Sens.* **2023**, 919−932.
(37) Varun, D. N.; Manjunatha, J. G.; Hareesha, N.; Sandeep, S.; Mallu, P.; Karthik, C. S.; Prinith, N. S.; Sreeharsha, N.; Asdaq, S. M. B. Simple and Sensitive Electrochemical Analysis of Riboflavin at Functionalized Carbon Nanofiber Modified Carbon Nanotube Sensor. *Monatshefte für Chemie.* **2021**, *152* (10), 1183−1191.

(38) Sanjay, B.P.; Sandeep, S.; Santhosh, A.S.; Karthik, C.S.; Varun, D.N.; Kumara Swamy, N.; Mallu, P.; Nithin, K.S.; Rajabathar, J. R.; Muthusamy, K. Unprecedented 2D GNR-CoB Nanocomposite for Detection and Degradation of Malachite Green - A Computational Prediction of Degradation Pathway and Toxicity. *Chemosphere.* **2022**, *287*, 132153.
(39) Hareesha, N.; Soumya, D. M.; Mounesh; Manjunatha, J. G.; Rohit, R. N.; Manikanta, P.; Varun, D. N.; Ataollahi, N.; Thippeswamy, B. A.; Pramoda, K.; Nagaraja, B. M. Honeycomb Polypore Biomass-Derived Activated Porous Carbon Nanosheets/Graphite/Nafion Composite: Green and Sensitive Electrocatalyst for Nanomolar Detection of Hg^{2+} Ions and Water-Splitting Reactions. *J. Environ. Chem. Eng.* **2024**, *12* (5), 113584.
(40) Knott, L. M.; Long, E.; Garner, C. P.; Fly, A.; Reid, B.; Atkins, A. Insights Into Lithium-Ion Battery Cell Temperature and State of Charge Using Dynamic Electrochemical Impedance Spectroscopy. *International Journal of Energy Research* **2024**, *2024* (1), 9657360.
(41) Swaby, S.; Monzón, D.; Ureña, N.; Vivo Vilches, J.; Sanchez, J. Y.; Iojoiu, C.; Várez, A.; Pérez-Prior, M. T.; Levenfeld, B. Block Copolymer-Based Membranes for Vanadium Redox Flow Batteries: Synthesis, Characterization, and Performance. *ACS Appl. Polym. Mater.* **2024**, *6* (15), 8966−8976.
(42) Lou, X.; Lu, B.; He, M.; Yu, Y.; Zhu, X.; Peng, F.; Qin, C.; Ding, M.; Jia, C. Functionalized Carbon Black Modified Sulfonated Polyether Ether Ketone Membrane for Highly Stable Vanadium Redox Flow Battery. *J. Membr. Sci.* **2022**, *643*, 120015.
(43) Li, X.; Ye, T.; Liu, W.; Meng, G.; Guo, W.; Grigoriev, S. A.; He, D.; Sun, C. Sulfonated Poly(Ether Ether Ketone)-Zirconia Organic-Inorganic Hybrid Membranes with Enhanced Ion Selectivity and Hydrophilicity for Vanadium Redox Flow Batteries. *Polymers.* **2025**, *17*, 2287.
(44) Niu, R.; Kong, L.; Zheng, L.; Wang, H.; Shi, H. Novel Graphitic Carbon Nitride Nanosheets/Sulfonated Poly(Ether Ether Ketone) Acid-Base Hybrid Membrane for Vanadium Redox Flow Battery. *J. Membr. Sci.* **2017**, *525*, 220−228.
(45) Zhang, Y.; Wang, H.; Qian, P.; Zhang, L.; Zhou, Y.; Shi, H. Hybrid Proton Exchange Membrane of Sulfonated Poly(Ether Ether Ketone) Containing Polydopamine-Coated Carbon Nanotubes Loaded Phosphotungstic Acid for Vanadium Redox Flow Battery. *J. Membr. Sci.* **2021**, *625*, 119159.
(46) Huang, X.; Nakagawa, S.; Houjou, H.; Yoshie, N. Insights into the Role of Hydrogen Bonds on the Mechanical Properties of Polymer Networks. *Macromolecules.* **2021**, *54* (9), 4070−4080.
(47) Park, C. H.; Lee, C. H.; Guiver, M. D.; Lee, Y. M. Sulfonated Hydrocarbon Membranes for Medium-Temperature and Low-Humidity Proton Exchange Membrane Fuel Cells (PEMFCs). *Prog. Polym. Sci.* **2011**, *36* (11), 1443−1498.
(48) Shaari, N.; Kamarudin, S. K. Recent Advances in Additive-Enhanced Polymer Electrolyte Membrane Properties in Fuel Cell Applications: An Overview. *Int. J. Energy Res.* **2019**, *43* (7), 2756−2794.
(49) Mayadevi, T. S.; Goo, B. H.; Paek, S. Y.; Choi, O.; Kim, Y.; Kwon, O. J.; Lee, S. Y.; Kim, H. J.; Kim, T. H. Nafion Composite Membranes Impregnated with Polydopamine and Poly(Sulfonated Dopamine) for High-Performance Proton Exchange Membranes. *ACS Omega.* **2022**, *7* (15), 12956−12970.
(50) Nujud Badawi, M.; Kuniyil, M.; Bhatia, M.; Kumar, S. S. A.; Mrutunjaya, B.; Luqman, M.; Adil, S. F. Recent Advances in Flexible/Stretchable Hydrogel Electrolytes in Energy Storage Devices. *J. Energy Storage.* **2023**, *73*, 108810.

https://doi.org/10.1021/acsapm.5c03977
ACS Appl. Polym. Mater. 2026, 8, 2653−2661